No. O-050

The Impact of a Wind Farm with Doubly-Fed Induction Generator on the Power Grid

NAJAFI, Hamid Reza, SAMADI, Ali Asghar and DASTYAR, Farshad
Department of Electric Power System, Faculty of Engineering, University of Birjand, IRAN

ROBINSON, Francis
Department of Electronic and Electrical Engineering, University of Bath, U.K

Abstract

This paper studies the impact of wind farm operation with doubly-fed induction generator (DFIG) connected to grid from a different point of view. Two configurations are investigated: i) grid and load alone, and ii) grid, load and wind farm. The important characteristics such as voltage profile, load bus PV characteristic, active power losses, and also transient stability at no load, full load and different fault conditions (three-phase symmetrical short circuit and one phase-to-ground short circuit) are studied for connected and unconnected wind-farm operation. The simulation results show that the connection of a DFIG improves the grid voltage stability. The reason is the capability of the DFIG to supply reactive power to the grid. The DFIG harmonic problems are also analyzed and undesirable effects of rotor side converter on the system were presented. A suitable filter is designed, analyzed and proposed for reduction of system THD.

Keywords: Doubly-Fed Induction Generator (DFIG), wind farm, transient stability, harmonic distortion

1 INTRODUCTION

As a result of conventional energy sources consumption and increasing environmental concern, efforts have been made to generate electricity from renewable sources, such as wind energy sources. Institutional support on wind energy sources, together with the wind energy potential and improvement of wind energy conversion technology, has led to a fast development of wind power generation in recent years. Other reasons could be the fuel price but especially environmental demands. The wind generation does not pollute the surrounding areas and also does not produce waste products.

To get the maximum possible power, the wind generator speed should change according to the wind speed [1]. Generally the Wind turbines (WTs) can either operate at fixed speed or variable speed. For a fixed speed wind turbine the generator is directly connected to the electrical grid. The rotor speed of the fixed-speed wind turbine is in principle determined by a gearbox and the pole-pair number of the generator. An impediment of the fixed speed Wind turbine is that power quality of the output power is poor. For a variable speed wind turbine equipped with a converter connected to the stator of the generator, the generator could either be a cage-bar induction generator, synchronous generator or permanent-magnet synchronous generator. There are several reasons for using variable-speed operation of wind turbines; among those are possibilities to reduce stresses of the mechanical structure, acoustic noise reduction and the possibility to control active and reactive power [2].

An important type of variable speed wind turbine is wind turbine with doubly-fed induction generator (WT-DFIG). This means that the stator is directly connected to the grid while the rotor winding is connected via slip rings to a back-to-back converter (see Fig.1.A). Today, doubly-fed induction generators are commonly used by the wind turbine industries for larger wind turbines [3]. The major advantage of the DFIG, which has made it popular, is that the power electronic equipment only has to handle a fraction (20–30%) of the total system power [4,5]. This means that the cost of the power electronic equipment and the losses in the equipment can be reduced in comparison to power electronic equipment that has to handle the total system power as for a direct-driven synchronous generator, apart from the cost saving of using a smaller converter. [6]

The rest of this paper is organized as follows: section 2 describes WT-DFIG model consist of turbine, drive train, pitch controller, generator, converter controller models. Section 3 explains the study system. The results of simulation are presented in section 4. Conclusions are finally made in section 5.

2 WIND TURBINE WITH DFIG

For variable-speed systems with limited variable-speed range, e.g. ±30% of synchronous speed, the DFIG can be a cost-effective solution [7]. The DFIG converter consists of two converters that are connected "back-to-back" as in Figure 1; machine-side converter and grid-side converter. Between the converters a dc-link capacitor is placed, as energy storage to keep the dc-link voltage variations (or ripple) small. With the machine-side converter it is possible to control the torque or the speed of the DFIG and also the power factor at the stator terminals, while the main objective for the grid-side converter is to keep the dc-link voltage constant. The speed–torque characteristics of the DFIG system can be seen in Figure 2 [4]. As also seen in the figure, the DFIG can operate both in motor and generator operation with a rotor-speed range of $\pm\Delta\omega_r^{max}$ around the synchronous speed, ω_1.

2.1 WT-DFIG Model Description

The complete model of a **WT-DFIG** is constructed from a number of sub models, i.e. a) turbine, b) drive train, c) pitch controller, d) wound-rotor induction generator, e) rotor-side converters. The general structure of the model is in Fig. 1.a.

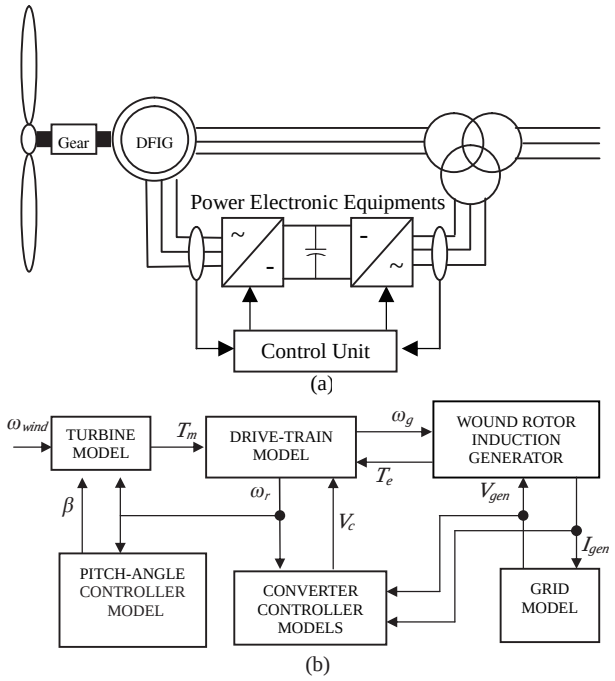

Figure 1. a) General structure of the DFIG, b) DFIG sub-models interrelations.

A) Turbine model

One common way to control the active power of a wind turbine is by regulating the c_p value of the rotor turbine. In the model, the c_p value of the turbine rotor is approximated using a non-linear function according to (2) [8].

$$p_{mech} = \frac{1}{2}\rho A_r C_p(\lambda,\beta)\omega_{wind}^{\ 3},\ \lambda = \frac{\omega_r r_r}{\omega_{wind}} \qquad (1)$$

$$c_p(\lambda,\beta) = 0.22\left(\frac{116}{\lambda_i} - 0.4\beta - 5\right).e^{\frac{-12.5}{\lambda_i}} \qquad (2)$$

$$\frac{1}{\lambda_i} = \frac{1}{\lambda + 0.008\beta} - \frac{0.035}{\beta^3 + 1} \qquad (3)$$

Where C_p is the power coefficient, β is the pitch angle, λ is the tip speed ratio, ω_{wind} is the wind speed, ω_r is the rotor speed, r_r is the rotor-plane radius, ρ is the air density and A_r is the area swept by the rotor.

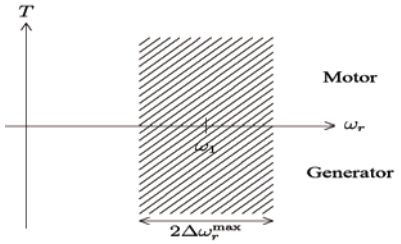

Figure 2. Speed–torque characteristics of a DFIG.

B) Drive-train model

When investigating dynamic stability, it is important to include the drive-train system of a wind turbine in the model. Its model consists of two main masses; the turbine mass and generator mass (Figure 3). These are connected to each other via a shaft that has certain stiffness and damping constant values. The equation of the turbine side is given as:

$$2H_t\frac{d\omega_t}{dt} = T_t - K_S.\theta_{tg} - D_S.(\omega_t - \omega_g) \qquad (4)$$

$$2H_g\frac{d\omega_g}{dt} = T_g + K_S.\theta_{tg} + D_S.(\omega_t - \omega_g) \qquad (5)$$

$$\frac{d\theta_{tg}}{dt} = \omega_{base}(\omega_t - \omega_g) \qquad (6)$$

Where H is the inertia constant, T is torque and ω is angular speed. Subscripts g and t indicate the generator and turbine quantities, respectively. The shaft stiffness and damping constant value are represented in K_S and D_S, ω_{base} s in the base value of angular speed [9].

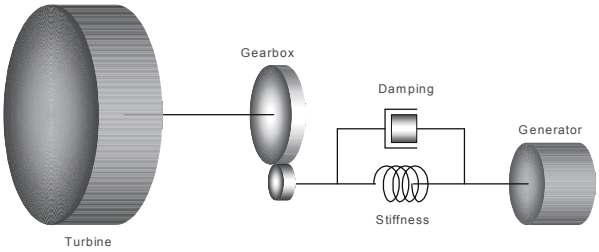

Figure 3. Drive- Train system of **WT-DFIG.**

C) Pitch controller model

According to Equation (2), the c_p value can be reduced by increasing the pitch angle β. However, the pitch angle is not

able to reach the set point value immediately. Accordingly, for a more realistic simulation, a rate limiter is implemented in the pitch controller model. The pitch-angle controller block diagram, shown in Figure 4, is employed to limit the rotor speed. For this reason, the pitch-angle controller is active only during high average wind speed [9].

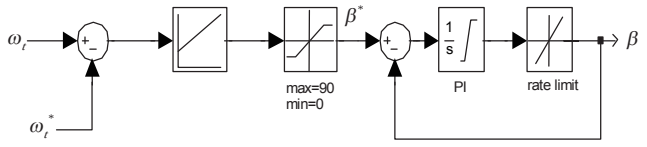

Figure 4. Pitch controller diagram.

D) Generator model

The generator is basically a slip-ring induction machine, which can be modeled according to [10] by the following equations.

$$u_s = R_s.i_s + \frac{d}{dt}(\psi_s) + (\omega_a - \omega_s)\psi_s \qquad (7)$$

$$u_r = R_r.i_r + \frac{d}{dt}(\psi_r) + (\omega_a - \omega_r)\psi_r \qquad (8)$$

where u, i and ψ are vectors of voltage, current and flux those are functions of time, and R is the resistance. Subscripts s and r denote the stator and rotor quantities. The speed of the rotor is denoted by ω_r. The equations are given in an arbitrary reference frame, which rotates at arbitrary speed of ω_a. The flux and current relations are given as

$$\psi_s = (L_{sl} + L_m).i_s + L_m.i_r \qquad (9)$$

$$\psi_r = (L_{rl} + L_m).i_r + L_m.i_s \qquad (10)$$

where L_m is the mutual inductance and L_{sl} and L_{rl} are the stator and rotor leakage inductances, respectively.

E) The rotor side converters controller model

The rotor side converter is modeled as a voltage source type. For simplification, switching phenomena and dynamic limitations in the converter are neglected by assuming that switching frequency is infinite. The purpose of the controller is to regulate the active and reactive power output independently. To decouple these two parameters, generator quantities are calculated using vector control in a synchronous reference frame fixed to the stator flux. The controller provides set-point values of the quadrature and direct axis component of the rotor current (i_{qr} and i_{dr}). The active power is controlled as shown in Figure 5 [11].

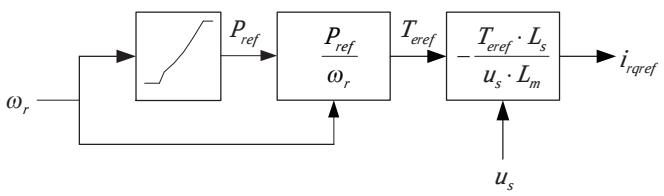

Figure 5. Active power control diagram.

A generic model of the voltage and reactive power control is arranged in a cascaded mode as shown in Figure 6 [12].

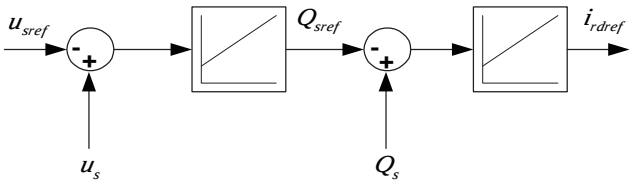

Figure 6. Reactive power and voltage control diagram.

The DFIG can be operated to implement, either constant reactive power control, or controlled terminal voltage. In this paper, the first method is employed.

3 SYSTEM UNDER STUDY

The system studied is a 24kV radial distribution system connected to the main utility grid via a short transmission line as shown in Figure 7. It comprises three buses, i.e. the wind-farm bus, load bus and grid bus. The wind-farm bus is equipped with six 1.5 MW WT-DFIGs that are connected via a 24 kV, 15km long, transmission line to the load bus. The load and WT-DFIG data are taken from [9].

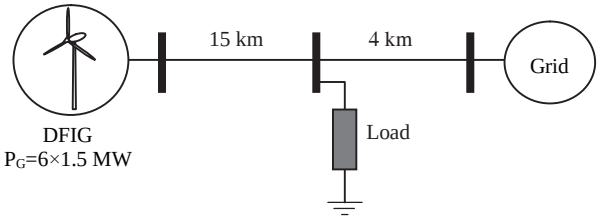

Figure 7. Single-line diagram of the study system.

4 SIMULATION

To investigate the impact of operating the WT-DFIG on the power grid, two configurations are distinguished: i) grid and load alone, and ii) grid, load and wind farm. The important characteristics, such as voltage profile, load bus PV characteristic, active power losses, and also transient stability at no load, full load and different fault conditions (three-phase symmetrical short circuit and one phase-to-ground short circuit) are studied for connected and unconnected wind-farm operation.

4.1 Steady State Voltage Profile

The steady-state voltage profile for two different conditions are simulated, a) wind farm connected at wind speeds of 4 m/s , 8 m/s, 12 m/s (nominal generation), and 20 m/s, and b) wind farm is not connected. Load-bus voltage at non presence of wind-farm bus, is represented in (11) and (12).

$$V_{loadbus} = \cos\theta\, V_{grid} - jZ_c \sin\theta\, I_{grid} \qquad (11)$$

$$I_{grid} = \frac{p_{grid} - jQ_{grid}}{V^*_{grid}} \qquad (12)$$

From equations (11) and (12):

$$V_{loadbus} = \left[\cos\theta - jP^*_{grid}\sin\theta - Q^*_{grid}\sin\theta\right]V_{grid} \qquad (13)$$

With $P^*_{grid} = \frac{P_{grid}}{P_c}, Q^*_{grid} = \frac{Q_{grid}}{P_c}$ where $V_{loadbus}$ is the load-bus voltage, θ is the wave length, Q_{grid}, P_{grid} are the grid reactive and active powers respectively, P_c is the natural power, V_{grid} is the grid voltage and Z_c is the natural impedance. By considering equation (13), if Q^*_{grid} or P^*_{grid} reduce, $V_{loadbus}$ will improve. Figure 8 shows the simulation results.

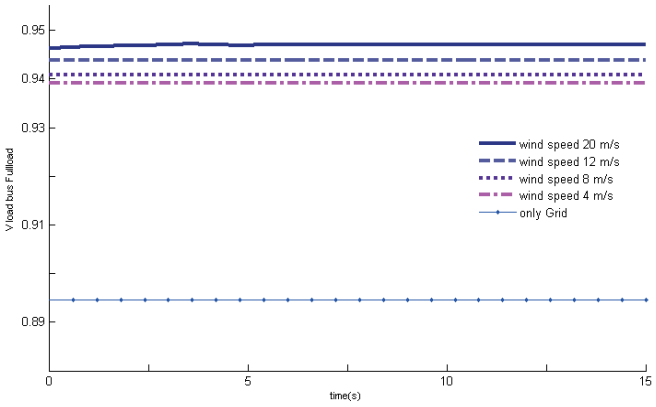

Figure 8. Steady-state voltage profile for conditions (a) and (b)

The wind-farm bus injects the active and reactive power to the load bus and improves the load-bus voltage. By increasing the wind speed, the $V_{loadbus}$ improvement is greater.

4.2 Voltage stability (PV characteristics)

By considering Figure 7, the following equations can be obtained for the connected wind farm:

$$V_{grid} = V_{load}\cos\theta + jZ_c\sin\theta\, I_{load} \qquad (14)$$

with $I_{load} = \frac{P_{load} - Q_{load}}{V^*_{load}}$.

$$V_{load}V_{grid} = V^2_{load}\cos\theta + jZ_c\sin\theta\left(P_{load} - jQ_{load}\right) \qquad (15)$$

$$V^4_{load}\cos^2\theta + V^2_{load}\left(Q_{load}Z_c\sin 2\theta - V^2_{grid}\right) + Z^2_c\sin^2\theta\left(P^2_{load} + Q^2_{load}\right) = 0 \qquad (16)$$

$$AV^4_{load} + BV^2_{load} + C = 0 \qquad (17)$$

with $A = \cos^2\theta,\ B = \left(Q_{load}Z_c\sin 2\theta - V^2_{grid}\right),$
$C = Z^2_c\sin^2\theta\left(P^2_{load} + Q^2_{load}\right)$

$$V_{load} = \pm\sqrt{\frac{-B \pm \sqrt{B^2 - 4AC}}{2A}} \qquad (18)$$

Regarding equations (14) to (18), increasing the reception of active and reactive powers from the grid, decreases the voltage stability of the load bus. The PV characteristics are shown at Figures 9 and 10. These curves are obtained at different wind speeds for connected and unconnected wind-farm operation. The results also show improvement of load-voltage stability at the connected wind farm using DFIGs.

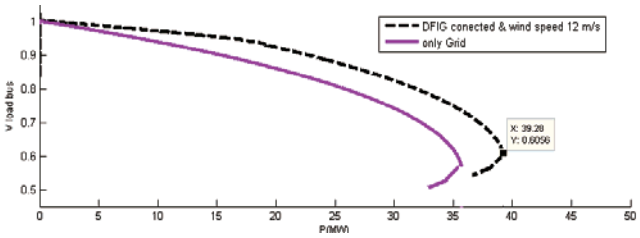

Figure 9. PV curves for 12m/s wind speed under connected and unconnected wind-farm conditions

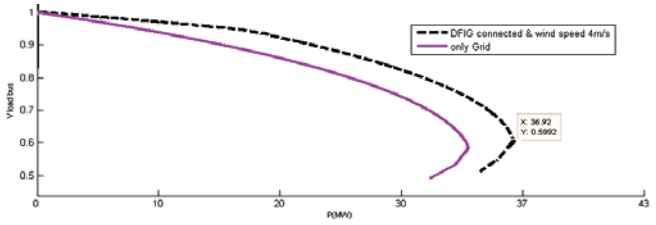

Figure 10. PV characteristics for 4m/s wind speeds under connected and unconnected wind-farm conditions

4.3 Line Active Power Losses

Active power loss in the transmission line can be calculated by the equations (19) to (21).

$$P_{loss\_line} = 3\times Z_{line}\times\left|I_{grid}\right|^2 \qquad (19)$$

According to: $I_{grid} = \frac{P_{grid} - jQ_{grid}}{V^*_{grid}}$

$$P_{loss\_line} = 3\times Z_{line}\times\frac{\left|P^2_{grid} + Q^2_{grid}\right|}{\left|V_{grid}\right|^2} \qquad (20)$$

Total active power losses under full-load and no-load conditions at different wind speed (4, 8, 12, and 20m/s) are calculated according to equation (21).

$$P_{Total\ Loss} = P_{grid} + P_{DFIG} - P_{load} \qquad (21)$$

Where $P_{Total\ Loss}$ is the total line power losses, P_{grid} the grid delivered power, P_{DFIG} the wind-farm delivered power and P_{load} the power consumed by the load. According to equation (20), any reduction in P_{grid} or Q_{grid}, reduces the power losses. This reduction of P_{grid} or Q_{grid} may be compensated by the wind farm. Figure 11 gives simulation results.

As the results show, with full-load the active losses reduce when the wind speed increases due to an increasing injected power from the wind farm. In contrast, with no-load an increasing wind speed raises the losses. The reason for this is the lengthy power transmission lines between the wind farm and grid. (see equation (20))

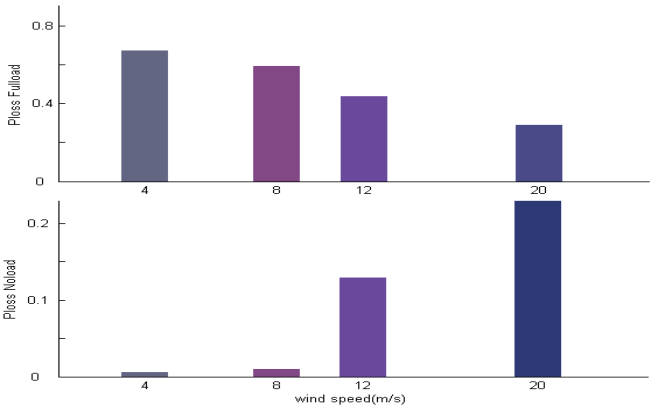

Figure 11. Active power losses at full load and no-load

4.4 Transient Stability

For transient-stability evaluation a series of simulations are performed considering different operating conditions. The following scenarios are examined: i) applying a short-circuit fault that is cleared after 200 ms, ii) connecting and disconnecting load, iii) wind-turbine operation under the fault condition, iv) wind turbines operation for the connected load condition ,v) wind turbine operation with disconnection from the wind-farm bus. At t = 5s, a temporary three-phase short-circuit is placed on the load bus. After fault clearing, the load is disconnected from the load bus. The load is connected again at t = 6.2s. Simulation results are shown in figures 12 and 13. During faults all the DFIG turbines have zero outputs; but, after fault clearance, all of them experience short-term motor behavior. This is due to energy attraction by the turbines. For briefness, only two-turbine behavior is presented in the figures. However, the system becomes stable after a short time.

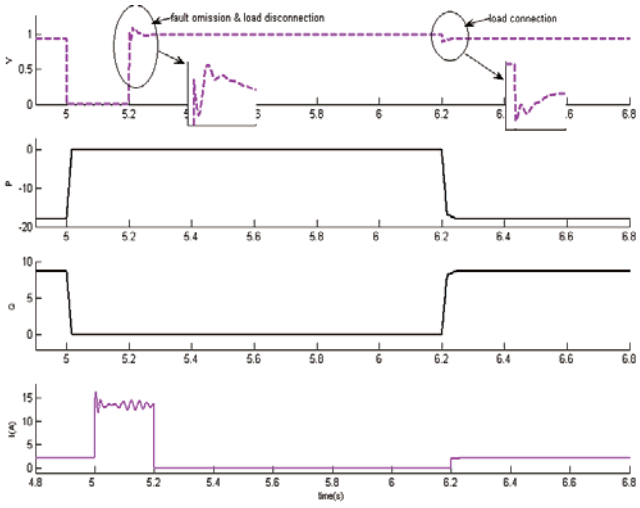

Figure 12. Three-phase fault on the load bus

WTs-DFIG operation during local load connection is also investigated and results are shown at figure 14. This figure consists of the wind-farm voltage, active and reactive power, the rotor speeds of the two turbines, and their pitch angle variations during this condition. The WT rotor speeds as a transient stability indicator show a stable behavior. Finally, figure 15 shows the result when one of the WT-DFIG is disconnected from the wind farm.

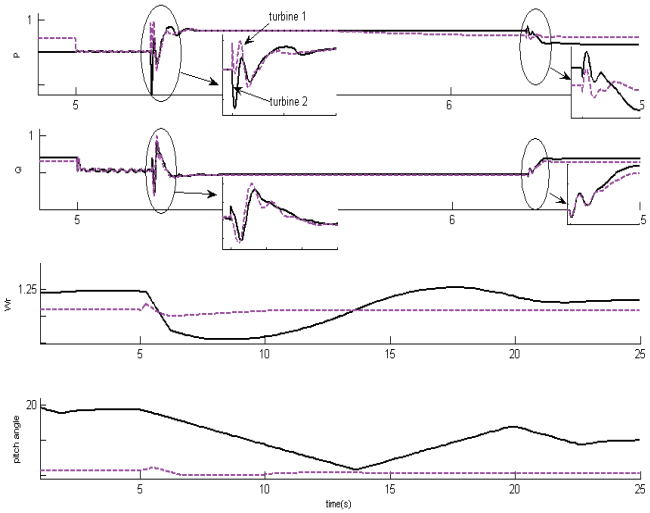

Figure13. WTs-DFIG operation for three-phase fault condition

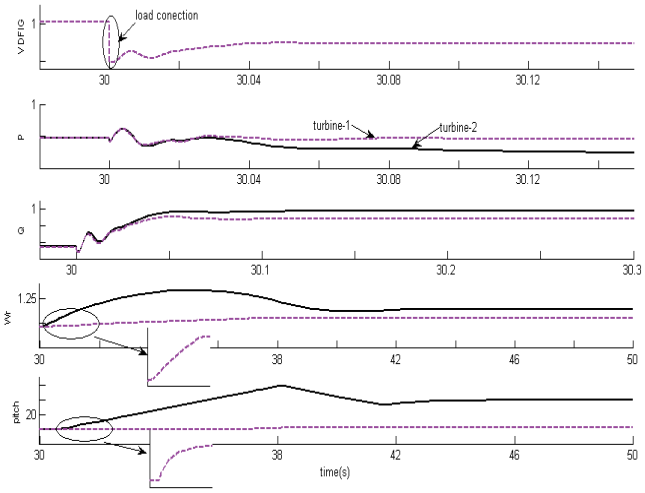

Figure 14. WTs-DFIG operation for load-connected condition

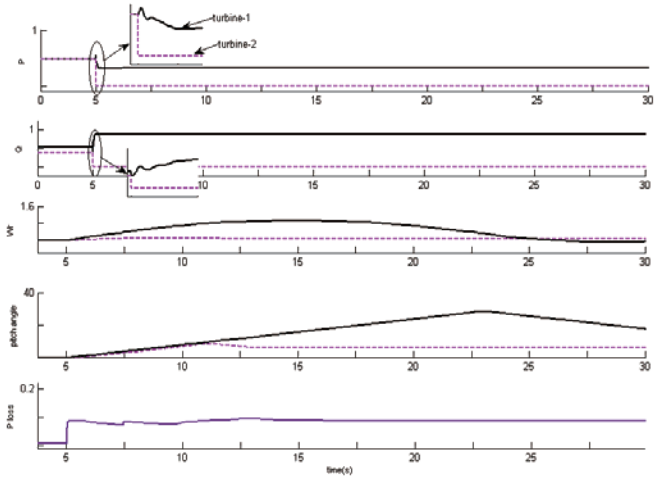

Figure 15. Turbine disconnection condition

4.5 Harmonic Analysis

It is important to limit the levels of harmonic-current injected into power systems by wind-farm power converters to minimize the likelihood of any disturbance to the operation and sizing of grid components and other grid-connected equipment. It is advisable to aim for an overall harmonic distortion level below that specified by StdIEEE 519 [13], for example. This paper uses the total harmonic distortion factor as a harmonic indicator. Current harmonic distortion is produced by the DFIG converters. The THD factor is defined according to equation (21), where I_1 is the fundamental component.

$$\text{THD}_{\text{i}} = \frac{\sqrt{\sum_{n=2}^{N} I_n^2}}{I_1} \qquad , N = 3,4,5,.... \tag{21}$$

The harmonic distortion of the current and the voltage arises because of the switched-mode nature of the DFIG-rotor power-converters. The simulation results in figure 16 show that approximately 6.44% THD arises when the wind farm with DFIG is connected, so filter installation is necessary. A suitable filter is designed and installed and reduces THD to approximately 1.44%. This shows that in the event of the harmonic pollution of WT-DFIG exceeding recommended levels, filter installation is necessary and effective.

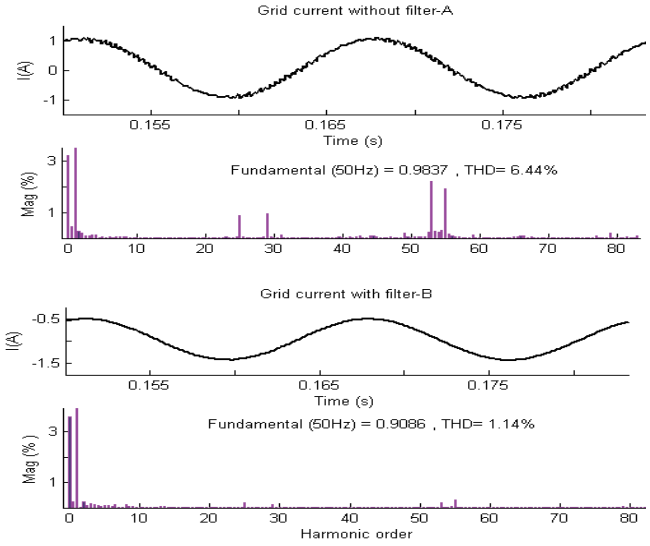

Figure 16. Harmonic content of grid current with and without filter with the presence of a DFIG

4 CONCLUSIONS

The research and simulation results have shown that the WT-DFIG improves the voltage profile and the voltage stability of the load bus. In addition, this impact is confirmed at low wind speed 4m/s (low generation). During faults all the DFIG turbines have zero outputs; but after fault clearance all of them experience short-term motor behavior; however the system remains stable after that. In general, the connection of WT-DFIGs improve the stability of the system and the load voltage. Wind power generation with DFIG provides better performance for terminal-voltage recovery after the load connects suddenly. The DFIG harmonic problems were also analyzed and the undesirable effects of the rotor-side converter on the system were presented. A suitable filter was designed, analyzed and proposed for reduction of system THD.

REFERENCES

[1] T. Burton, D. Sharpe, N. Jenkins, and E. Bossanyi, "Wind Energy Handbook". John Wiley & Sons, 2001.

[2] GE Wind Energy. (2005, Jan) 3.6s Offshore wind turbine Brochure. Available: http://www.gepower.com/prodserv/products/windturbines/en/downloads/ge36brochure.pdf

[3] Nordex, (2005, Jan.) N80/2500 kW N90/2300 kW. Brochure. Available: http://www.nordex-online.com/e/onlineservice/download/dateien/PB N80 GB.pdf

[4] L. H. Hansen, et al, "Conceptual survey of generators and power electronics for wind turbines", Risoational Laboratory, Roskilde, Denmark, Tech. Rep. Risø-R-1205(EN), ISBN 87-550-2743-8, Dec. 2001

[5] L. Xu , C. Wei, "Torque and reactive power control of a doubly fed induction machine by position sensorless scheme," IEEE Trans. Ind. Applicat., vol. 31, no. 3, pp. 636–642, May/June 1995.

[6] L. Morel, et al, "Double-fed induction machine: converter optimisation and field oriented control without position sensor", IEE Proc. Electr. Power Appl., vol. 145, no. 4, July 1998, pp. 360–368.

[7] F. M. Hughes, et al, "Control of DFIG-based wind generation for power network support," IEEE Trans. on Power Syst. , vol. 20, no. 4, 2005, pp. 1958-1966.

[8] S. Heier, "Grid Integration of Wind Energy Conversion Systems". John Wiley & Sons Ltd. 1998.

[9] A. Perdana, O. Carlson, and J. Persson, "Dynamic Response of Grid-Connected Wind Turbine with Doubly Fed Induction Generator during Disturbances", Nordic Workshop on Power and Industrial Electronics, TRONDHEIM – 2004.

[10] P.K. Kovács, "Transient Phenomena in Electrical Machines". Elsevier, New York, 1984.

[11] A. Perdana, "Dynamic Modeling of Wind Power Generation with Doubly Fed Induction Generator", B-EES-0302. Master Thesis Report. Royal Institute of Technology. Stockholm 2003.

[12] V. Akhmatov, "Modeling of Variable-speed Wind Turbines with Doubly-Fed Induction Generators in Short-Term Stability Investigations", Proc. of Workshop on Transmission Networks for offshore wind farms, Stockholm. April 2002.

[13] "IEEE Guide for Harmonic Control and Reactive Compensation of Static Power Converters", IEEEstd 519.